THE JOURNAL OF COMPARATIVE NEUROLOGY 443:56–70 (2002)

Connection From Cortical Area V2 to MT in Macaque Monkey

JOHN C. ANDERSON* **AND KEVAN A.C. MARTIN***
Institute for Neuroinformatics, University of Zürich and ETH Zürich, Winterthurerstr. 190 8057 Zürich, Switzerland

ABSTRACT

The extrastriate visual area of the macaque monkey called MT or V5, receives its input from multiple sources. We have previously examined the synaptic connections made by V1 cells that project to MT (Anderson et al., 1998). Here, we provide a similar analysis of the projection from V2 to MT. The major target of the V2 projection in MT is layer 4, where it forms clusters of asymmetric (excitatory) synapses. Unlike the V1 projection, it also forms synapses in layers 1 and 2 and does not form synapses in layer 6. The most frequently encountered targets of boutons labeled from V2 were spines (67% in layer 4; 82% in layer 2/3). Unusually, only 5/12 boutons examined in layer 1 actually formed synapses. Unlike the V1 projection, multisynaptic boutons were rare (mean, 1.1 synapses per bouton vs. 1.7 for the V1 projection). Like the V1 projection, the input to MT from any point in V2 is sparse (contributing approximately 4–6% of the asymmetric synapses in the densest clusters in layer 4). The synapses of the V2 projection were similar in size to those of the V1 projection (0.1 μm^2 vs. 0.09 μm^2) and both formed more complex postsynaptic densities on spines than on dendritic shafts. The clear differences between the V1 and V2 projection to MT indicate that their functions are complementary rather than completely overlapping. J. Comp. Neurol. 443: 56–70, 2002.

Indexing terms: visual cortex; area MT; corticocortical; light and electron microscopy; synapse morphology; postsynaptic target

The interconnections between cortical areas have been intensively explored in the primate since anatomists began their concerted effort to trace these pathways at the end of the 1960s. The extensive database that has since emerged has been used to develop models of the basic circuits of primate visual cortex, the most prominent of which are hierarchical models (Rockland and Pandya, 1979; Friedman, 1983; Maunsell and Van Essen, 1983; Felleman and Van Essen, 1991; Young, 1992; Jouve et al., 1998; Sporns et al., 2000; Barone et al., 2000) that use differences in the laminar patterns of interconnections to define projections as feedforward, lateral, or feedback. The anatomic studies have also formed the critical mass of data that has been crucial for the functional exploration of extrastriate visual cortex and for interpreting the results from human functional imaging studies. In their extreme simplification, the convenient divisions into feedforward, feedback, and lateral may obscure subtle but important differences between projections in a particular division. To explore this possibility, we compare here the connections made by two feedforward projections with the same target area MT.

We have previously examined, at light and electron microscopic level, the projection from V1 to MT, so for comparative purposes, we made a similar analysis of the projection from V2 to MT. The neurons that are the source of this V2 projection have been identified by retrograde transport of tracers (Lund et al., 1981; Maunsell and van Essen, 1983; Ungerleider and Desimone, 1986). They are pyramidal cells located mostly in layer 3B, with some scattered in layers 2, 3A, and 5. With anterograde tracers and light microscopy, Rockland (1995) found that both V1 and V2 axons terminate in the middle layers of MT, but unlike the V1 axons, the V2 axons do not form collateral

Grant sponsor: The EU; Grant number: QULG3-1999-01064; Grant sponsor: HFSP; Grant number: RG0123/2000-B; Grant sponsor: Swiss National Science Foundation.

*Correspondence to: John G. Anderson and Kevan A.C. Martin, Institute for Neuroinformatics, University of Zürich and ETH Zürich, Winterthurerstr.190, 8057 Zürich, Switzerland. E-mail: kevan@ini.phys.ethz.ch

Received 30 July 2001; Revised 10 October 2001; Accepted 23 October 2001

DOI 10.1002/cne.10100

projections in layer 6. A subsequent electron microscopic analysis (Anderson et al., 1998) indicated that the synapses formed in MT by the V1 axons are mainly with spiny dendrites (80%), with the remainder being with somata and dendrites of smooth neurons The large terminal boutons of the V1 afferents in MT were multisynaptic and formed morphologically heterogeneous synaptic specializations. The results of the present study indicate that, although there are basic similarities between the two projections, in that both have a dominant input to excitatory neurons in layer 4 of MT, there are sufficient points of difference to suggest that the feedforward pathways may be interestingly heterogenous in the fine structure and function of their connections.

MATERIALS AND METHODS

The material presented here was taken from two adult female macaque monkeys (*Macaca mulatta*). Animals were prepared for surgery after the administration of an intramuscular premedication of xylazine (Rompun, Beyelar, 0.5 mg/kg)/ketamine (Ketalar, Parke Davis, 10 mg/kg). This was followed by cannulation of a femoral vein for the delivery of alphaxalone/alphadalone (Saffan, Glaxo) to establish complete anaesthesia. Sterile surgery was carried out in accordance with the guidelines of the Cantonal Veterinary Authority of Zürich.

Each animal received pressure injections (~0.5 μl each) of the neuronal tracers biotinylated dextran amine (BDA; Molecular Probes, Leiden, The Netherlands) and *Phaseolus vulgaris* leucoagglutinin (PHA-L; Vector Laboratories, Burlingame, CA). One animal received four injections of 10% BDA in 0.01 M phosphate buffered saline pH 7.4 (PBS) and two of PHA-L in 10 nM phosphate buffer pH 7.4 (PB). The second animal received five and three injections of the above, respectively. After a 14-day survival period, the animals were very deeply anesthetized with i.v. pentobarbital (20 mg/kg) and then perfused transcardially with a normal saline solution, followed by a solution of 4% paraformaldehyde, 0.3% glutaraldehyde, and 15% picric acid in 0.1 M PB pH 7.4. The brain was removed from the skull, and a block of cortex containing the injection site and area MT was removed. The block was allowed to sink in sucrose solutions of 10, 20, and 30% in 0.1 M PB. Sections were cut from the block at 80 μm in the parasagittal plane and collected in 30% sucrose in 0.1 M PB. The sections were then freeze-thawed in liquid nitrogen and washed in 0.1 M PB. We used standard procedures to reveal the neuronal tracers. In brief outline; washes in PBS were followed by 10% normal swine serum (NSS) in PBS (1 hour). The antibody to PHA-L was diluted in the above at 1:200 and exposed for 48 hours at 5°C. Further washes in NSS preceded overnight exposure (5°C) to an avidin-biotin complex (Vector ABC kit-Elite). The peroxidase activity was identified by using 3,3-diaminobenzidene tetrahydrochloride (DAB). After assessment by light microscopy, selected regions of tissue were treated with 1% osmium tetroxide in 0.1 M PB. Dehydration through alcohols (1% uranyl acetate in the 70% alcohol) and propylene oxide allowed flat mounting in Durcupan (Fluka) on glass slides.

Light microscopic observations of labeled axons were carried out to locate and select regions of interest for electron microscopy. We reconstructed individual collaterals in the less densely innervated areas for correlated light and electron microscopy. Serial ultrathin sections were collected at 70-nm thickness on Pioloform-coated single-slot copper grids. Labeled boutons were photographed at a magnification of 21,000. Synapses and associated structures were classified by using conventional criteria. Collections of serial sections were digitized and reconstructed by using Trakem, an in-house EM-digitization package. To measure and display the postsynaptic densities of labeled boutons, we used software developed by ourselves which has been described in outline elsewhere (see Materials and Methods section; Anderson et al., 1998).

The estimates of labeled bouton density were derived by using the physical disector method (Sterio, 1984). We selected regions of particularly dense innervation by labeled axons for re-embedding. Serial 70-nm-thick sections were collected from these regions and a "reference" and "look-up" section was selected. The reference and look-up sections were separated by one section. Photomicrographs were taken with the electron microscope to form strips of tissue, 12 to 16 images abutted together, or patches of tissue, e.g., 2 × 8 images. All electron photomicrographs were taken at 11,500× magnification. Synapses that were in the reference section, but that disappeared in the look-up section were counted. Synapses that were present in both look-up and reference sections were not counted (Sterio, 1984). However, all photographed labeled synapses were used in some part of the following analysis.

RESULTS

Light microscopy

Each of two monkeys received pressure injections of BDA and PHA-L into area V2 (area 18) along the crest of the lunate gyrus (Fig. 1A). With one exception, needle tracks were all confined to the gray matter of V2 and could be followed through all laminae (Fig. 1B). In one animal, the injections were made into the dorsal surface of V2, the needle track being almost parallel to the cortical laminae. Penetrations made in the second animal traversed the tip of the gyrus and extended into the lunate sulcus (e.g., Fig. 1B). One track in this animal went through the white matter. The resulting label spread over 5–7 mm mediolaterally. BDA labeling was poor at the injection site, but PHA-L labeling was excellent. Labeling was densest along the path of the penetrations. Most of the uptake was by pyramidal cells of layer 2/3, covering most of the tip of the gyrus, but labeled cell bodies were also found in layers 4, 5, and 6. Strong anterograde labeling was seen in striate and extrastriate visual areas, including MT, along with some pale-stained cell bodies (Fig. 2). The strongest transport was to V1, where the retrograde labeling was similar to that previously reported by Kennedy and Bullier (1985), i.e., predominantly in layers 2/3 and 4B, with some sparse cell bodies scattered along the layer 5/6 border. No cell or terminal labeling was evident in layer 4. Patches of labeled axons and palely stained cell bodies were also seen in the fundus and anterior bank of the lunate sulcus and in the posterior bank of the superior temporal sulcus. The distinctive myelination of MT was evident in the osmicated sections, and the labeled axons terminated at a point where MT forms a small bulge in the sulcus.

In area MT, the labeled axons entered from the white matter and sometimes branched as they passed through layers 5 and 6. On reaching layer 4, the axons branched

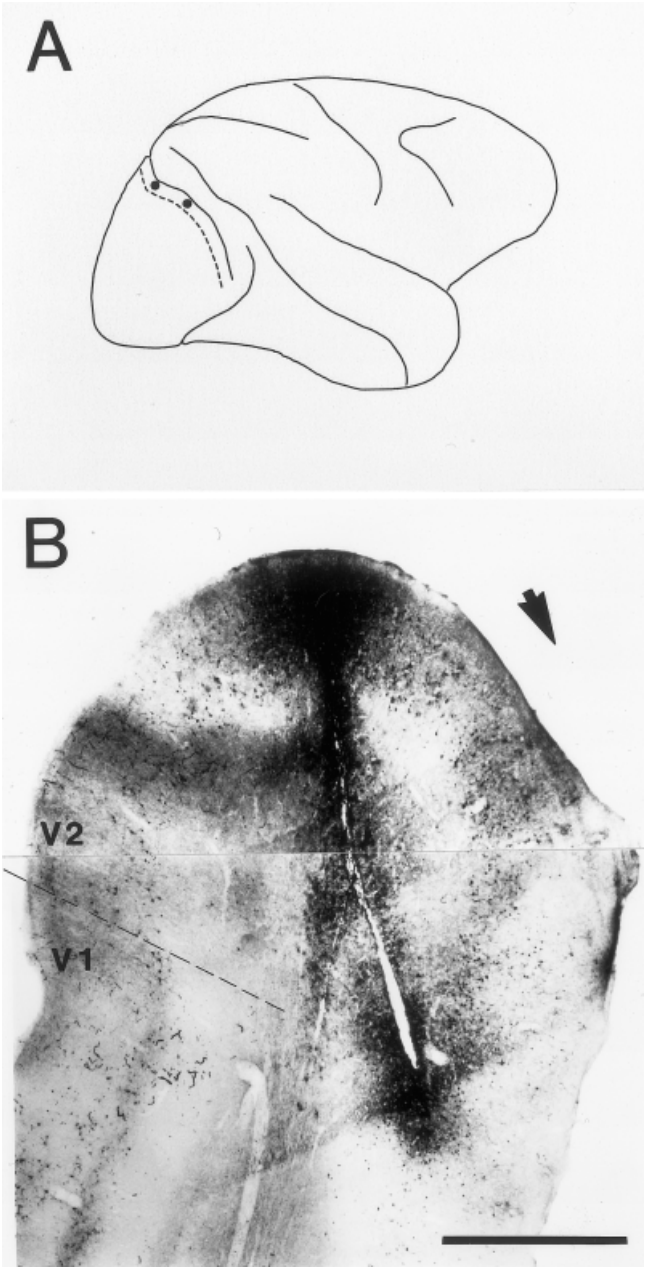

Fig. 1. Location of injection sites. **A:** Schematic drawing of macaque brain showing region in which injections were made (in zone between filled circles) along the edge of the lunate sulcus. The V1/V2 border is indicated by the dotted line. **B:** Photomontage of light photomicrographs of parasagittal section of the lunate gyrus showing an example of an injection site and label. The lunate sulcus is indicated by an arrow and the V1/V2 border by a dotted line. Scale bar = 1 mm in B.

extensively and formed synaptic boutons. This profusion of axons and both *en passant* and *terminaux* boutons gave an overall patchy appearance to the innervation site when viewed at low power in the light microscope (Fig. 2). The largest boutons were formed by axons with the thickest diameter, but bouton size and axon diameter was highly variable within layer 4.

Axons that projected into the more superficial layers were more slender than the main trunks seen in layer 4. They gave rise to *en passant* boutons of a fairly uniform size (Figs. 2, 4A,B) spaced at fairly regular intervals. Most of these axons terminated in or before upper layer 2/3. Occasionally thicker axons, passing through layer 3, branched before reaching layer 2 and produced a fanlike arborization. The axon diameter in these superficial layer axons reduced rapidly as they branched. A few axons could be followed up to the top of layer 2 and into layer 1 (Fig. 7). Axons that branched in layer 2 and sent a projection to layer 1 were fine and produced small, mostly *en passant* boutons. Axons that passed straight up to layer 1 without forming collaterals in layer 2 had larger boutons. Layer 1 had the poorest tissue quality for light and electron microscopy.

Weak retrograde labeling (Fig. 2) was evident by palely stained neuronal somata and proximal portions of the dendrites, in some instances. These cells were sparse and were clearly of a pyramidal morphology. The majority of retrogradely labeled somata occurred in layer 6 and 2/3. Less frequently somata could be seen within the elaborate tangle of anterograde labeled axon collaterals in layer 4. It was difficult to determine the nature of their morphology, pyramidal or stellate, due to the light staining of the somata and the intense staining of the labeled axon arbors arising from the anterogradely labeled V2 projection. The density of the labeling in layer 4 made it impossible to reconstruct at a light microscope level extensive portions of single axons. This density also made tight LM/EM correlation impossible. Thus, we selected for EM analysis areas of layer 4 with the densest labeling as determined in the light microscope. This sample included the greatest range of variation of bouton sizes for our EM study. The projections to the superficial layers were sparser and this enabled us to correlate light and electron microscopy.

Electron microscopy

We examined a total of 189 boutons from layers 1, 2/3, and 4 (12 from layer 1, 64 from layer 2/3, and 113 from layer 4). Of this sample, 133 boutons were serially sectioned and completely reconstructed and the remaining 56 were used for estimates of synaptic density, where we required only three sequential sections. A total of 199 labeled synapses were examined, all of which were asymmetric (Gray's type 1). We reproduced the electron photomicrographs of boutons from this study at approximately the same magnification as the images used in a previous study of V1 afferent boutons in MT (Anderson et al., 1998). This choice was made to facilitate a comparison of the two projections to MT.

The reaction end product was dark, although of variable intensity in different boutons. Vesicles and mitochondria were clearly visible inside the boutons and the synaptic clefts were not obscured by label. Myelinated axons were also labeled, confirming that the antibody had penetrated well, despite the insulating sheath. Small vacuoles formed in labeled structures (e.g., Figs. 3A,B, 5A). Most boutons were small (~0.5 μm diameter), compact structures containing one or two mitochondria and a cluster of vesicles over the region of the synaptic specialization (e.g., Figs. 3, 4, 6, 7). The synapse was indicated by the presence of presynaptic vesicles, a synaptic cleft and a postsynaptic density in the target structure. Occasionally, we saw a density within the labeled bouton that was mirrored by a

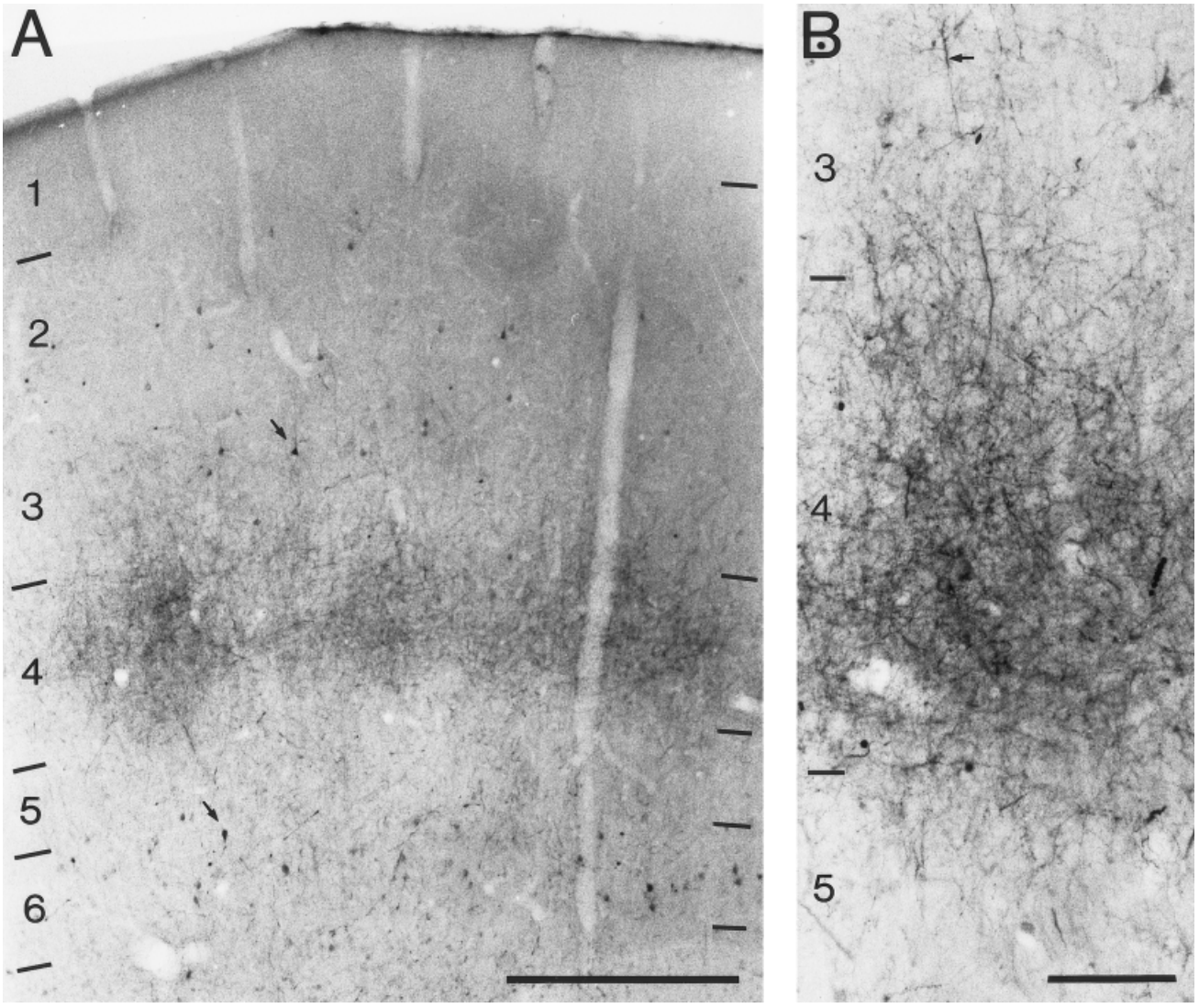

Fig. 2. Light photomicrographs of cortical area V5 showing *Phaseolus vulgaris* leucoagglutinin (PHA-L) -labeled axon termination zone. **A:** Labeled terminals form dense patches in layer 4 and lesser projections into layer 3. Laminae and their boundaries are indicated to the left and right. Lightly stained, retrogradely labeled cell bodies are located in layers 3 and 6 (small arrows). **B:** Adjacent section to A taken at higher-power magnification. The labeled fibres branch profusely in layer 4 to form a dense network of axon collaterals and terminals. Numerous small and large (small arrow) caliber axons can be seen projecting through superficial layer 3. Laminae and their boundaries are indicated to the left. Scale bars = 0.5 mm in A, 100 μm in B.

similar density within the target (Fig. 5A,B,C). In the immediate vicinity of the presynaptic density, there were no vesicles. This mirror-like configuration was always seen close or adjacent to a conventional asymmetric synapse and was classified as a *puncta adherens* (Peters et al., 1991). We did not include these *puncta* in our reconstructions or estimates and measurements of synapses.

Spines. Serially sectioning the bouton, synapse, and target structures greatly assisted in determining the type of target that formed synapses with the labeled boutons. We also used standard ultrastructural criteria to classify targets (Peters et al., 1991). The most frequent targets were small spines (Figs. 3, 4, 7). Occasionally, we were able to trace spines back to a parent dendrite (Fig. 3B). A second synapse from an unlabeled bouton was seen on six of the spines and, in all cases, was of a symmetric morphology (Gray's type 2) (Fig. 3C). Only one spine was of the short and neckless "sessile" variety. Spines were the sole targets of the five synapses found in layer 1. Spine synapses formed 58 of the 71 synapses examined in layer 2/3, and 81 of the 121 synapses identified in layer 4.

Dendrites. Dendrites were also the targets of labeled boutons. These were usually identified by reconstruction from serial sections or by the presence of mitochondria and microtubules. The majority of dendrites were of fairly small caliber (~0.5–1 μm diameter) (Fig. 3E,D). The larger diameter dendrites were more easily characterized, although more infrequent (Fig. 3F). By using serial sections, dendrites could be grouped into two classes. One class had little variation in diameter when reconstructed

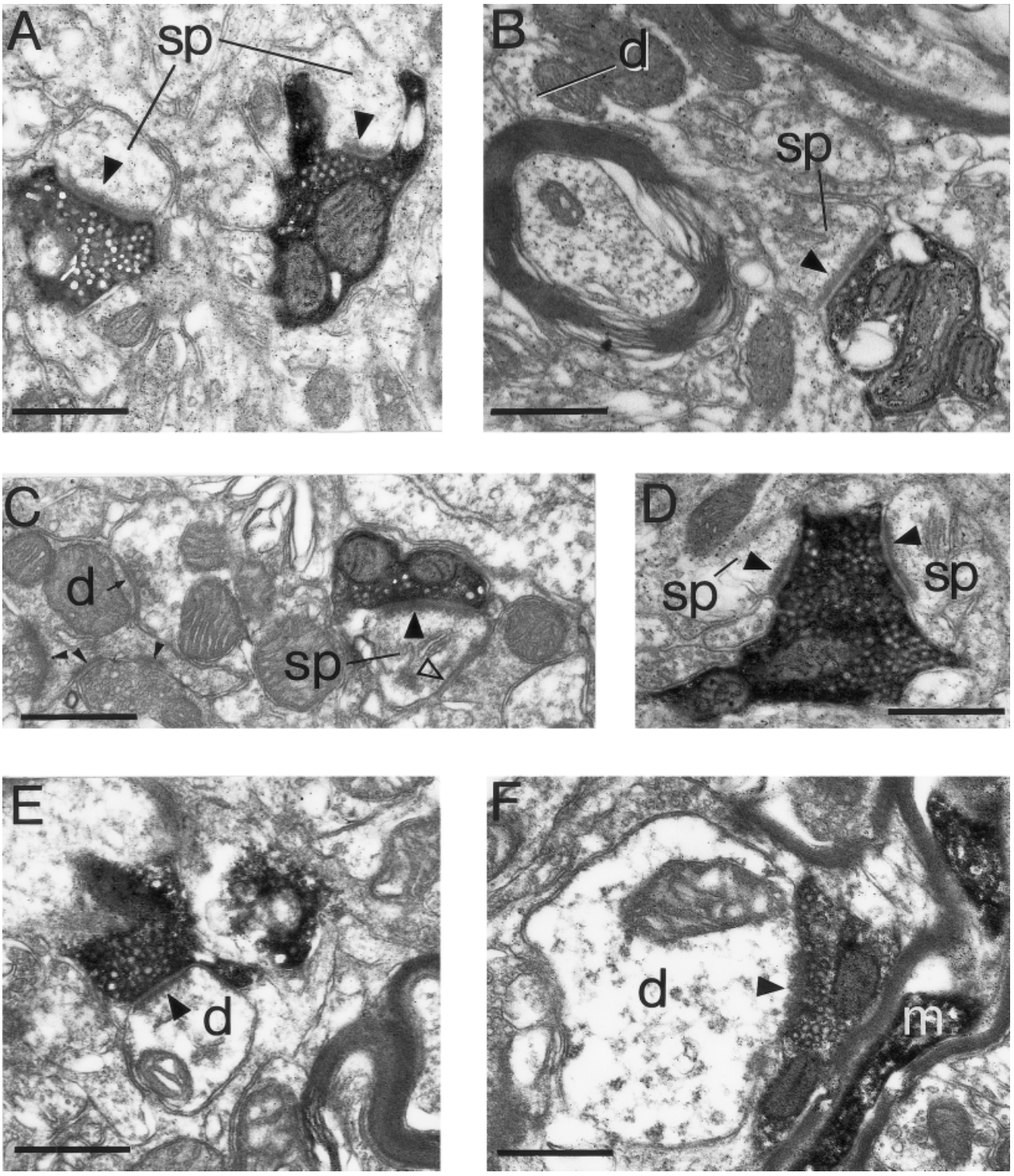

Fig. 3. Electron photomicrographs of *Phaseolus vulgaris* leucoagglutinin (PHA-L) -labeled electron dense axon and boutons located in layer 4 of area V5. A–D: Examples of synapses formed with spines. **A:** Two small boutons form asymmetric synapses (solid arrowheads) with spines (sp). This bouton/target configuration was characteristic of the majority of synaptic contacts seen in this study. Both boutons and their target spines have a small profile, the bouton contains at least one mitochondria and the remaining small space (usually above the synapse) is vesicle filled. **B:** A labeled bouton forms an asymmetric synapse (arrowhead) with a spine (sp), which can be traced back to the parent dendrite (d) within the same section. **C:** A spine forms an asymmetric synapse (large solid arrowhead) with a labeled bouton and a symmetric synapse (open arrowhead) with an unidentified bouton. A spine apparatus can be seen within the spine. For comparison of synapses within the same picture an unidentified dendrite (d) forms asymmetric (small solid arrowheads) and symmetric (small arrow) synapses with unidentified boutons. **D:** Two spines (sp) form asymmetric synapses (arrowheads) with a labeled bouton. The spine to the right contains a clearly identifiable spine apparatus. **E,F:** Examples of synapses formed with dendrites containing few mitochondria, forming synapses infrequently and showing little variation in diameter. These features are characteristic of neurons with spiny dendrites. **E:** A small caliber dendrite (d) forms an asymmetric synapse with a labeled bouton (arrowhead). **F:** A large caliber dendrite (d) forms an asymmetric synapse (arrowhead) with a labeled bouton. Adjacent to the bouton is a labeled myelinated axon (m). Scale bars = 0.5 μm in A–F.

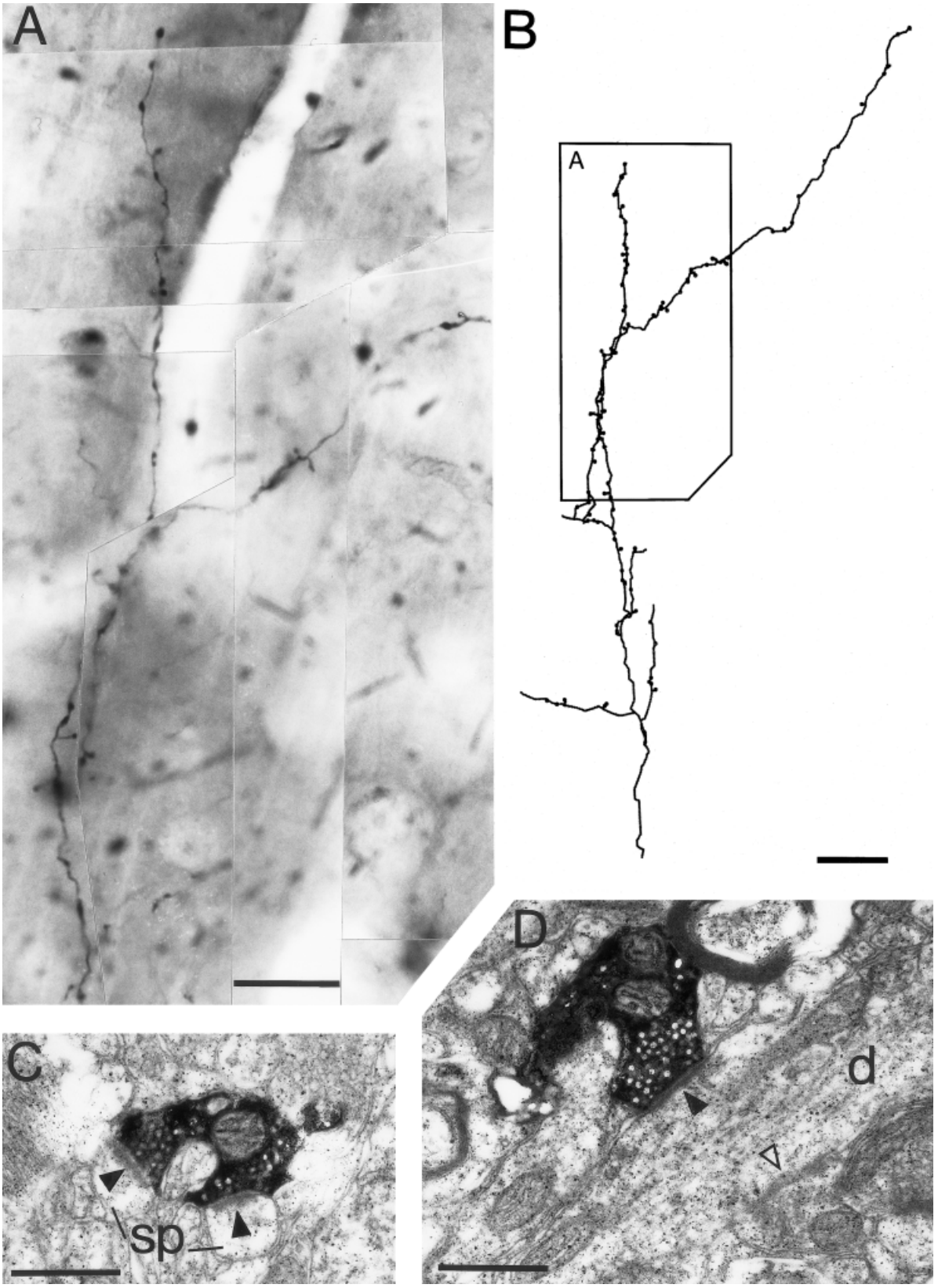

Fig. 4. Light and electron photomicrographs of *Phaseolus vulgaris* leucoagglutinin (PHA-L) -labeled axon and boutons located in layer 2/3. **A:** Photomontage of a single ascending collateral taken from the middle of layers 2 and 3. Numerous varicose swellings of the *en passant* and *terminaux* types can be clearly seen along the axon length. **B:** Light microscopic reconstruction of the collateral shown in A. The border between layers 1 and 2 is approximately 200 μm from the uppermost bouton, and the border between layers 3 and 4 is approximately 400 μm from the lowest point of the reconstructed axon. The box-shaped boundary represents the area shown in the photomontage (A). C,D: Electron photomicrographs of labeled boutons taken from the collateral shown in A. **C:** A small labeled bouton forms asymmetric synapses (arrowheads) with two spines (sp). **D:** A labeled bouton forms an asymmetric synapse (solid arrowhead) with a dendrite (d), and an unidentified bouton forms an obliquely sectioned symmetric synapse (open arrowhead) with the same dendrite. The dendrite shows little variation in diameter, forms synapses infrequently, and contains few mitochondria. Neurons with spiny dendrites show these features. Scale bars = 20 μm in A, 40 μm in B, 0.5 μm in C,D.

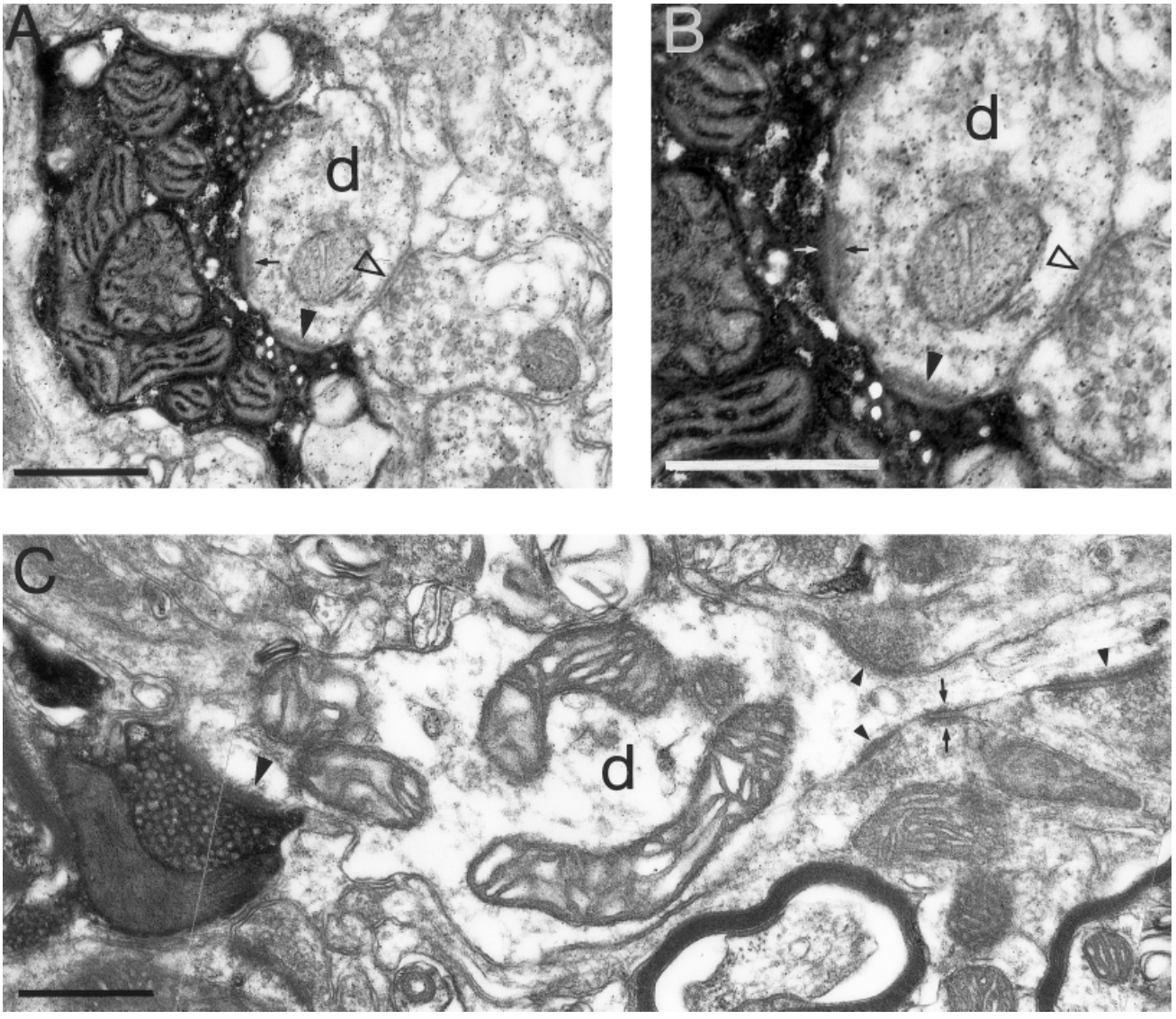

Fig. 5. Electron photomicrographs of *Phaseolus vulgaris* leucoagglutinin (PHA-L) -labeled boutons of layer 4 forming synapses with dendrites that contained numerous mitochondria, form many synapses, and have a smooth and beaded morphology. These are features associated with GABA-ergic neurons with smooth dendrites. The morphology of the dendrite was determined by serial section reconstruction. **A:** A large labeled bouton forms an asymmetric synapse (solid arrowhead) and a puncta adherens (small arrow) with a dendrite (d). The puncta appears as a density seen within the dendrite. It was situated adjacent to the asymmetric synapse and opposite the symmetric synapse. The dendrite also forms a symmetric synapse (open arrowhead) with an unidentified bouton. **B:** A higher-power photomicrograph of the dendrite (d) showing detail of the puncta and synapses indicated in B. The two synapses are indicated as in A. The puncta can be characterized by the density seen within the dendrite (black arrow) and a similar density within the labeled bouton (white arrow; the density appears gray against the black reaction product). Synaptic vesicles are clearly absent in the vicinity of the density within the bouton and present in the region presynaptic to the asymmetric synapse. **C:** A labeled bouton forms a synapse (large arrowhead) with a dendrite (d) that is of variable diameter. The dendrite contains several mitochondria within the segment of greatest diameter, and three asymmetric synapses (small solid arrowheads) form with unidentified boutons as the dendrite narrows rapidly. One of the boutons also forms a puncta (arrows) with the dendrite. Scale bars = 0.5 μm in A–C.

and formed few synapses, which is characteristic of the spiny dendrites of excitatory neurons. Six of the 12 dendritic synapses in layer 2/3 were of this variety and 9 of 19 of the completely reconstructed synapses in layer 4 were with spiny dendrites.

Another morphology of dendrite had a widely variable diameter (Fig. 5). A fortuitous plane of section along the length of such a dendrite make the changes in diameter obvious (Fig. 5C). In others, the varicose form of the dendrite was obvious after serial reconstruction. Such dendrites usually contained numerous mitochondria and even in single sections would form multiple synapses with other unidentified boutons. These dendrites are quite characteristic of neurons with smooth, varicose, or beaded dendrites that contain the inhibitory neurotransmitter GABA (Somogyi et al., 1983; Peters and Saint Marie, 1984; Kisvár-

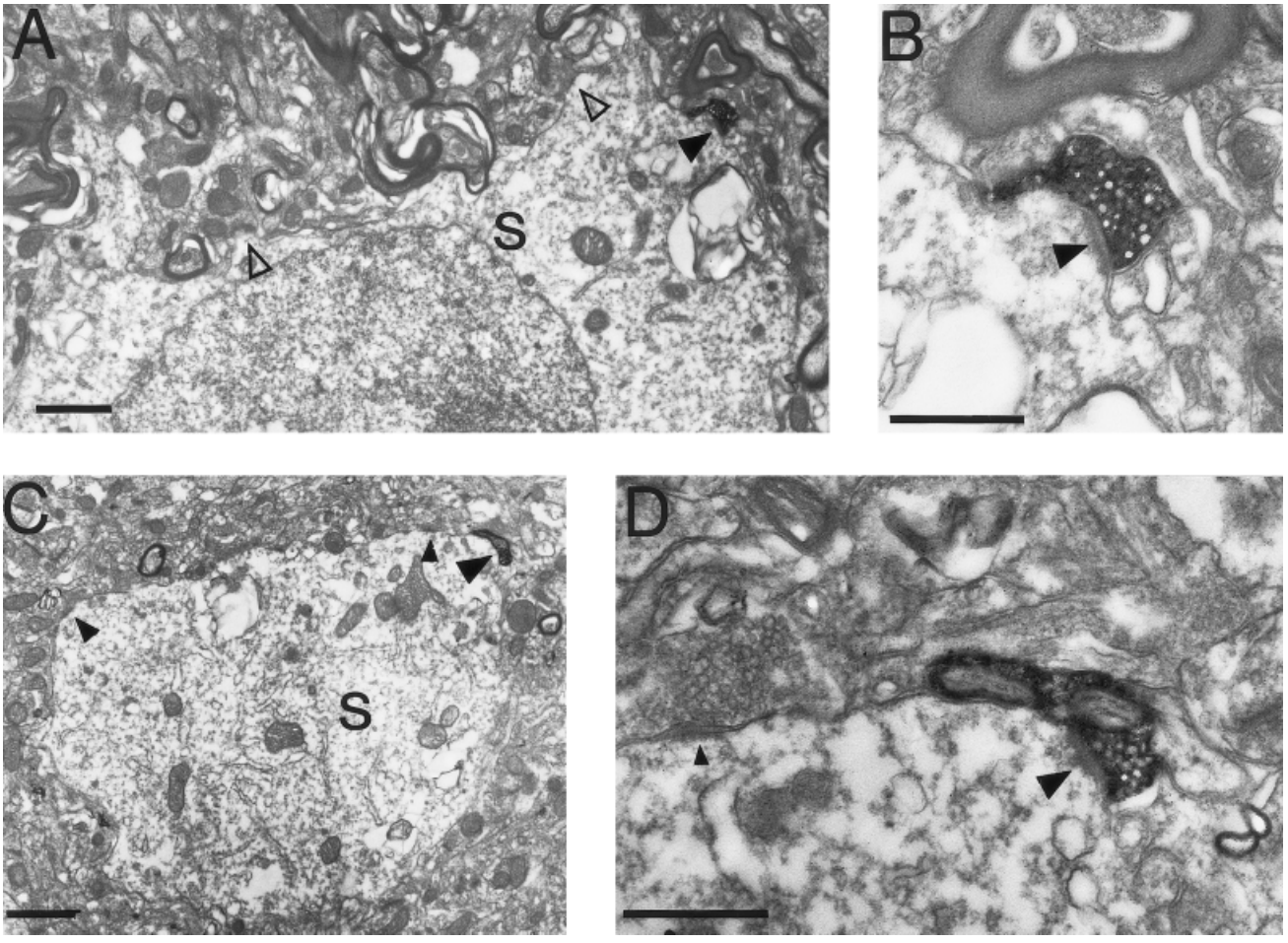

Fig. 6. Electron photomicrographs of labeled boutons in synaptic contact with soma. A,B: Bouton and soma from layer 4. **A:** Low-power electron photomicrograph of soma (s) forming an asymmetric synapse (solid arrowhead) with a small labeled bouton. The soma contains few mitochondria or organelles of the perikaryon and formed few synapses other than symmetric synapses (open arrowheads). These features are observed in excitatory neurons with spiny dendrites. **B:** High-power image of detail of the asymmetric synapse (solid arrowhead) indicated in A. **C:** Low-power electron photomicrograph of soma (s) from layer 3 in contact with labeled bouton (large arrowhead). The soma contained numerous mitochondria and perikaryal organelles as well as forming asymmetric synapses (small arrowheads) with unidentified boutons. These features are associated with γ-aminobutyric acid–containing neurons with smooth dendrites. **D:** High-power view of the adjacent section to that shown in C of the labeled bouton forming an asymmetric synapse (large arrowhead). For comparison of synapses, an adjacent asymmetric synapse (small arrowhead) formed by an unidentified bouton is included. Scale bars = 1 μm in A,C, 0.5 μm in B,D.

day et al., 1985; Ahmed et al., 1997). A surprisingly high proportion of serially reconstructed target dendrites had the features of smooth (GABAergic) neurons. In layer 2/3, 6 of 12 labeled synapses formed on these dendrites, and 10 of 19 synapses (52%) in layer 4 formed on smooth dendrites. By comparison, only 26% of the dendritic targets of the V1 projection to MT were smooth dendrites (Anderson et al., 1998). The only target that could be demonstrated to receive multiple synapses (3) from a labeled bouton was a smooth dendrite located in layer 2/3.

Somata. Only two neuronal somata were found to form synapses with labeled boutons (Fig. 6). Both of these synapses were from tiny boutons forming equally tiny synapses. One of these target soma was located in layer 4 and contained few mitochondria and organelles of the perikaryon and formed few synapses other than symmetric synapses. These features are generally attributed to neurons with spiny dendrites or excitatory neurons. The second soma was in layer 2/3. It contained numerous mitochondria, showed a lot of rough endoplasmic reticulum and formed asymmetric synapses with nonlabeled boutons. This finding is characteristic of a GABAergic cell soma, where asymmetric synapses on the soma are common.

Layer 1. We examined two axons projecting to layer 1 (Fig. 7). One axon showed labeling of a quality as we had seen in other laminae (left in Fig. 7A). The postsynaptic densities and synaptic clefts were clearly identified (Fig. 7B). The labeling of the second axon was very intense (right in Fig. 7A) and affected the structures surrounding the bouton. Only one bouton and its synapse could be used from this collateral (Fig. 7C). Only 5 of 12 of the optimally preserved boutons examined from layer 1 showed any synaptic specialization. However, the boutons all contained mitochondria and were filled with vesicles. The same collateral that provided most of the layer 1 data was

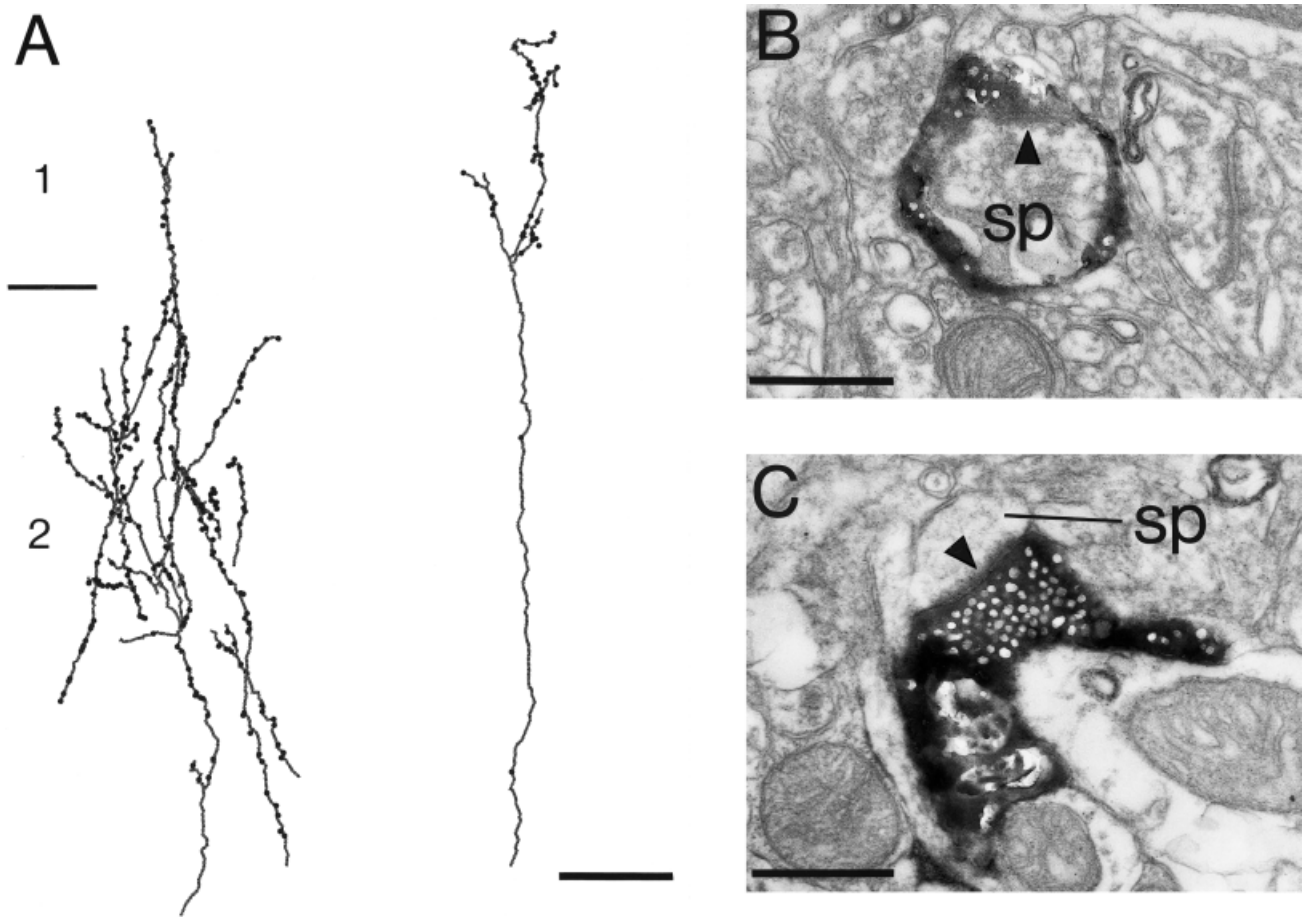

Fig. 7. Reconstructions and electron photomicrographs of the most superficially projecting *Phaseolus vulgaris* leucoagglutinin (PHA-L) -labeled axons. **A:** Two light microscopic reconstructions of axons projecting to layers 1 and 2. The axon on the left produces many collaterals and varicose swellings in layer 2 and continues with a smaller projection into layer 1. The axon on the right projects directly to layer 1 before producing collaterals or swellings. The laminae are indicated to the left. **B:** A labeled layer 1 bouton taken from the left-hand axon shown in A. The bouton forms an asymmetric synapse (arrowhead) with a spine (sp) and wraps around the circumference of the spine. **C:** A labeled layer 1 bouton taken from the right-hand axon shown in A forming an asymmetric synapse (solid arrowhead) with a spine (sp). Only half of the bouton swellings of layer 1 examined in the electron microscope formed synapses, although all were filled with vesicles. Scale bars = 10 μm in A, 0.5 μm in B,C.

also examined in layer 2. Six labeled boutons located slightly deeper (~10 μm) in the cortex at the border of layers 1 and 2 were examined and all formed synapses. Boutons in layer 1, synaptic or nonsynaptic, were also invaded by one or sometimes two nonlabeled structures, usually identifiable as boutons. All of the identified synaptic targets in layer 1 were spines.

Postsynaptic density. Reconstructing the bouton and its target gave us the opportunity to view the complete postsynaptic density as a two-dimensional (2-D) or 3-D structure. We have used this technique previously to obtain values of the surface area of synapses (Anderson et el., 1998). By focusing on the postsynaptic specialization rather than the presynaptic membrane, we avoided detail being obscured by reaction end-product in the bouton. We show a 2-D projection of the postsynaptic densities in Figure 8. There was no difference seen in the distributions of the areas of synapses made with the two main target types, spines and dendrites. Both had a mean of approximately 0.09 μm^2. When comparing synapses from different laminae, the distributions overlapped considerably (Fig. 9). Nevertheless, the layer 2/3 synapses were significantly smaller (mean, 0.076 μm^2; SEM, 0.004) than those of layer 4 (mean, 0.107 μm^2; SEM, 0.008) ($P = 0.0008$, two tailed t test). This significant difference was caused mainly by the higher frequency of very small synaptic areas seen in layers 2/3.

The postsynaptic density can be perforated giving it a doughnut or horseshoe morphology, as opposed to a simple disc. Figure 8 shows that the synapses with the more complex morphology are often formed with spines. A similar observation was made in the study of synapses made by V1 afferent boutons in area MT. However, the synapses formed by the V2 afferent boutons did not reach the degree of variety seen for the synapses of V1 boutons (Anderson et al., 1998). The mean size of the synapses of V2 in layer 4 (mean, 0.107 μm^2; SEM, 0.008) was slightly larger than that of the V1 boutons in layer 4 (mean, 0.093 μm^2; SEM, 0.007) (Fig. 10), but the difference was not significant ($P = 0.2$, two tailed t test). The synapses of V1

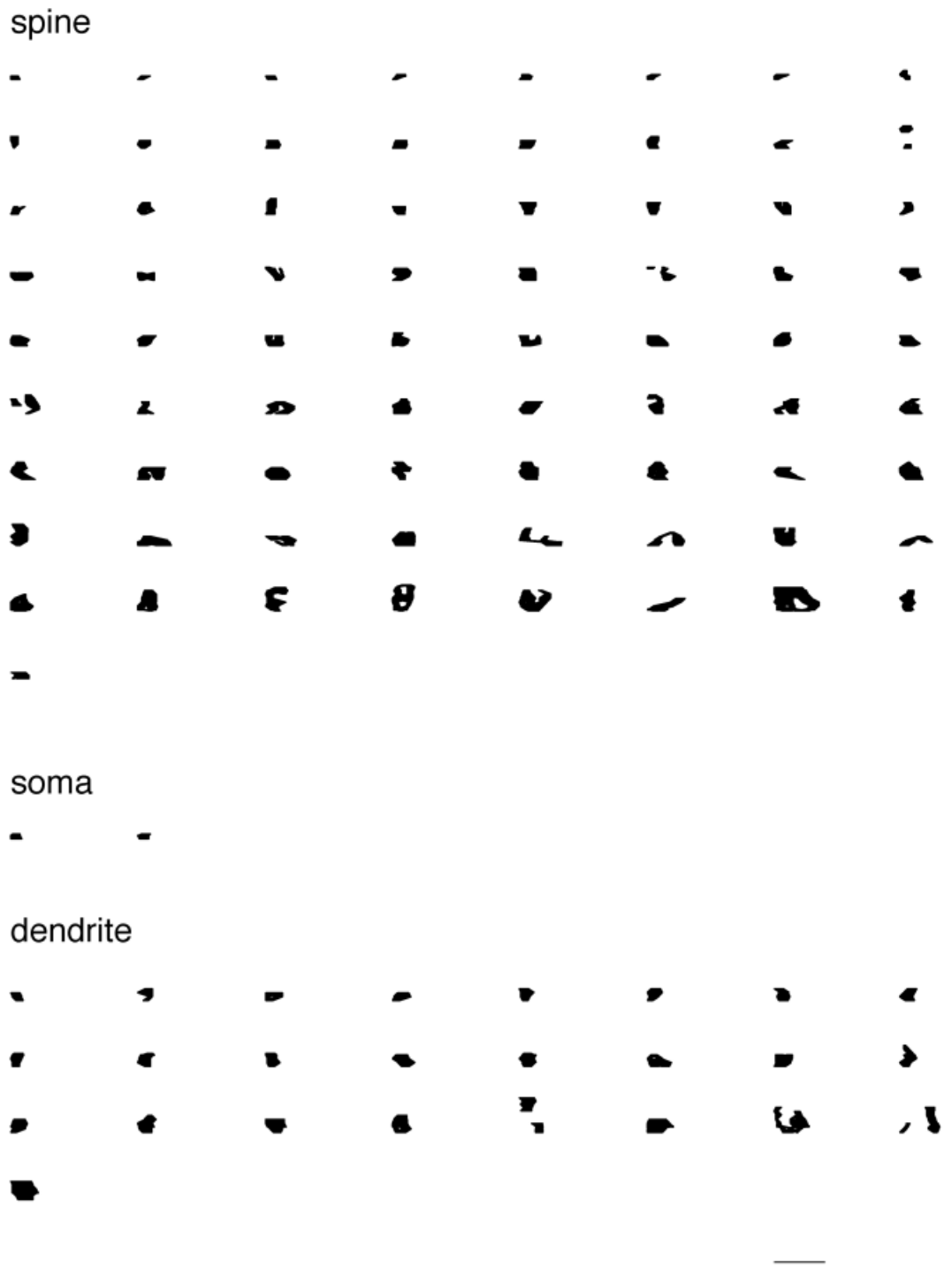

Fig. 8. Two-dimensional projection of the reconstructed postsynaptic densities found on spines, soma, and dendrites postsynaptic to V2-labeled boutons in area V5. The densities are ordered by increasing surface area. Scale bar = 1 μm.

boutons in MT tended to show more perforations. This condition gave the V1 synapses a more fragmented appearance. Some spines would form two synapses with V1 boutons, on opposite sides of the same spine head. The V1 synapses formed with somata were small, but beneath one bouton, there could be up to five separate active zones.

Target types. The most frequently encountered target of V2 labeled boutons were spines. The difference between boutons from the different principal laminae of innervation was the proportion of spines to dendrites as targets (Fig. 11). For this reason, we have not pooled the data from different laminae. In layer 4, 67% of the labeled

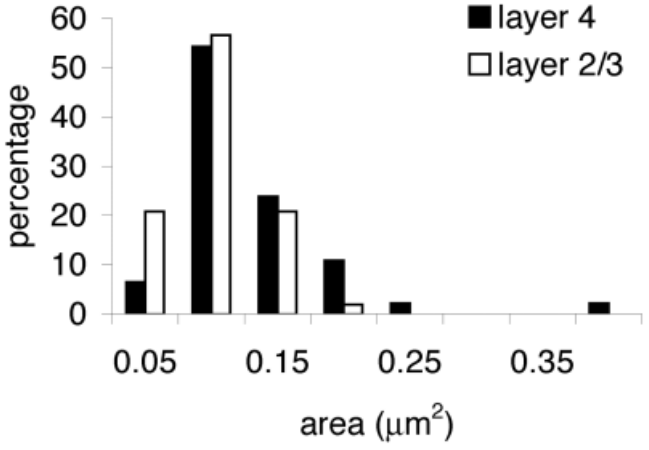

Fig. 9. Histogram of the distribution of postsynaptic areas (μm^2) formed by labeled V2 boutons in layers 2/3 (n = 53) and 4 (n = 46) of areaV5.

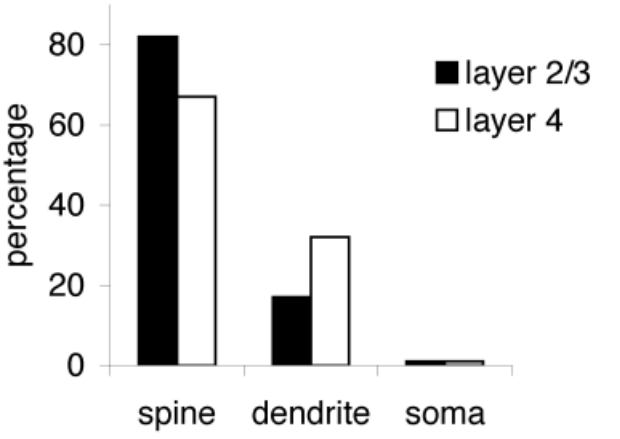

Fig. 11. Histogram of the synaptic targets of labeled V2 boutons in area V5. For layer 2/3, n = 53; for layer 4, n = 46.

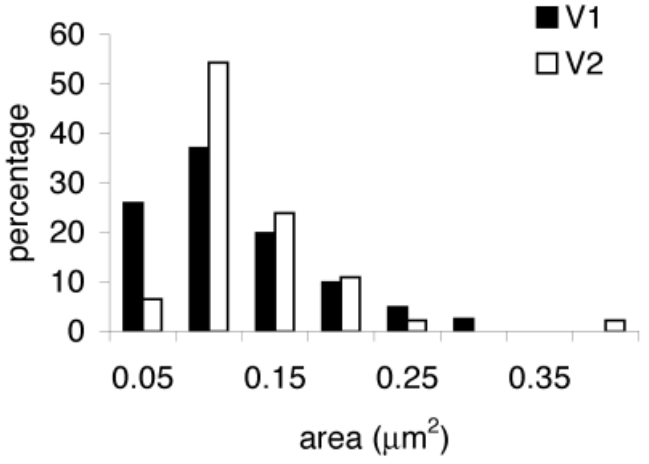

Fig. 10. Histogram of the distributions of postsynaptic areas (μm^2) formed by labeled V1 (n = 81) and V2 (n = 46) boutons in layer 4 of area V5.

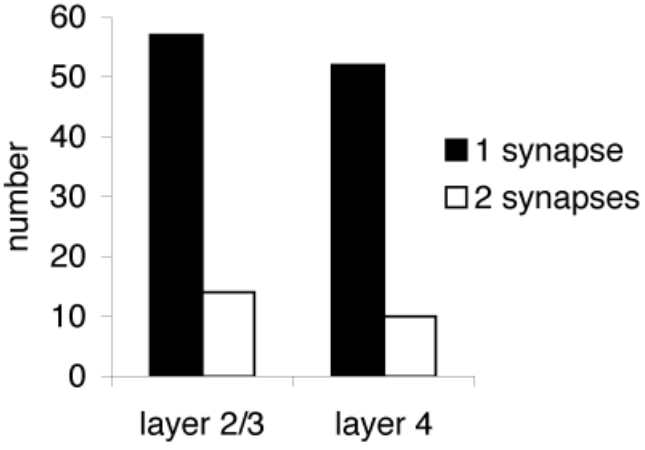

Fig. 12. Histogram of the number of synapses formed per labeled bouton in layers 2/3 and 4 of area V5.

synapses were formed with spines and 31% formed with dendritic shafts. This compares well with the quantitative disector analysis of layer 4, where we discovered that 65% of the targets that form asymmetric synapses were spines, with dendritic shafts forming the remaining 35% (n = 419). In layer 2/3, 82% of the synapses were formed with spines and 17% with dendritic shafts. A disector analysis was not made for layers 2/3. Neuronal somata accounted for approximately 1% of synaptic targets in both laminae. As indicated above (see *Dendrites*), smooth neurons provided approximately half of the dendritic shaft targets in layers 4 and 2/3. The two sections used for the disector analysis of layer 4 were too few to permit an accurate subdivision of the dendritic shafts into smooth and spiny types. Serial reconstructions indicated that most boutons made only one synapse and only rarely more than two synapses (Figs. 3D, 4C, 12). On average, there were 1.1 synapses per labeled bouton.

Synaptic density measurements. To estimate the relative proportion of synapses being contributed by V2 to area MT, we made an unbiased stereologic analysis of layer 4. We selected two sections from one animal in which the labeling was particularly dense. In Figure 2, we see that the terminal labeling in layer 4 has a patchy appearance. We selected regions from within the densest patches for our analysis by using the unbiased disector method (Sterio, 1984). We counted only those labeled synapses that disappeared in the "look-up" section when compared with a near adjacent "reference" section. Although the blocks of tissue used for re-embedding were selected from the densest zones of innervation, the distribution of labeled synapses in any ultrathin section could vary greatly. If the disector region was selected by using nonbiased features such as the edge of the tissue or a scratch on the block face, we counted no labeled synapses. If we selected the location of the disector by finding a labeled bouton and then sampling in the vicinity, we counted 5% (11 of 218) and 4.9% (10 of 205) of disappearing labeled synapses. The form of the disector altered the number of observations.

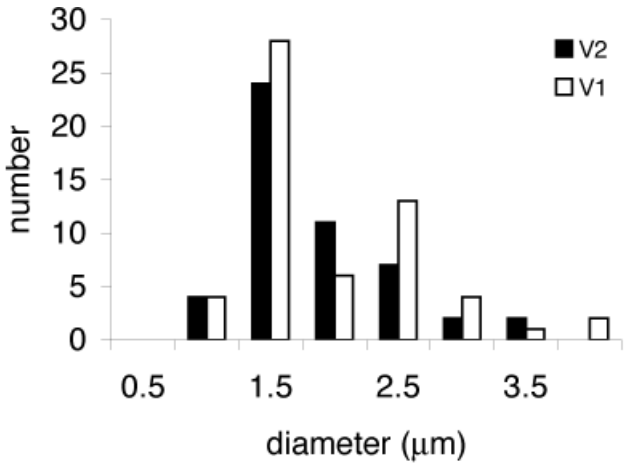

Fig. 13. Histogram of the distributions of diameters of labeled V1 and V2 axons near the border between the white matter and layer 6. All measurements were made with the light microscope by using a 100× oil immersion objective.

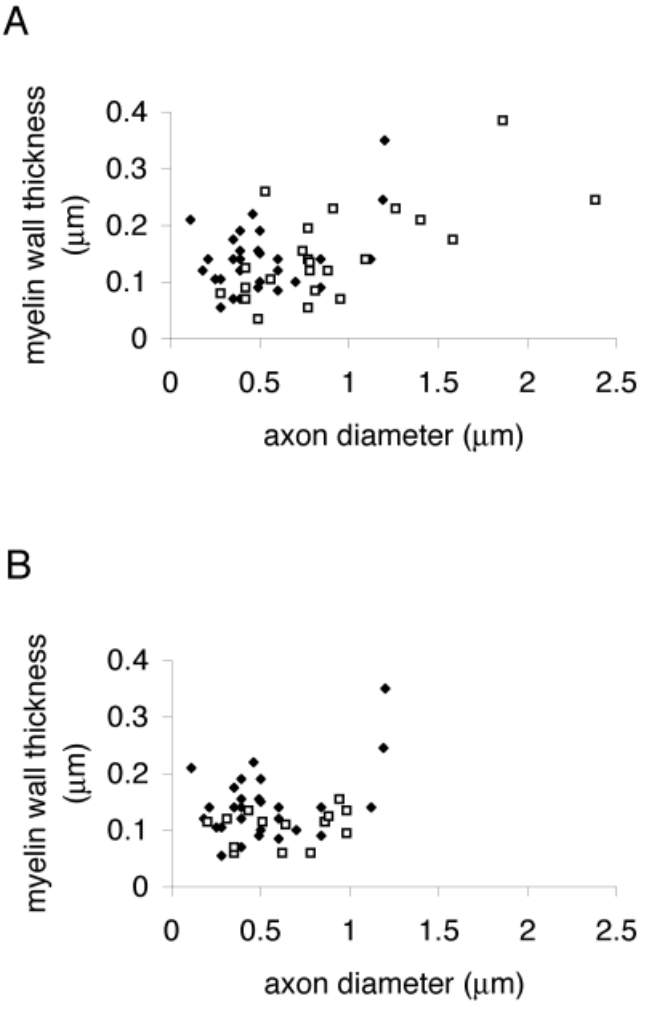

Fig. 14. Relationship between axon diameter and the thickness (μm) of the associated myelin sheath. All measurements were made in layer 4. **A:** Nonlabeled (open squares) and V2 labeled (filled diamonds) axons in area V5. **B:** Labeled axons in V5 originating from neurons located in areas V1 (open squares) and V2 (filled diamonds).

Strips of tissue tended to give lower values (3.8%; 8 of 211) than patches of tissue (6.2%; 13 of 211). This may indicate that even the most prolifically innervated regions of layer 4 have another, local level of "ultrastructural" organization.

Axons and myelin. The conduction times from V1 to MT are known (1.0–1.7 msec, Movshon and Newsome, 1996), but those for the V2 projection are not. As the axon diameter gives some indication of the relative conduction velocities of the axons, we compared the diameters of axons originating in V1 with those originating in V2. We measured in the light microscope the axon diameters of axons labeled from V1 and V2 as they entered MT but before they branched in the gray matter (Fig. 13). Axons originating in V1 and V2 have similar diameters. The terminal arbors also show a reduction in diameter, and this could also contribute significantly to the conduction times. We used electron microscopy to examine the diameters of the myelinated segments of the terminal arbors in layer 4 (Fig. 14) and found that again the V1 and V2 axons were comparable. These findings suggest that the axon conduction velocities of the two projections may be quite similar.

DISCUSSION

Both the V1 and the V2 projection to MT are classified as "feedforward" projections in that their dominant target is layer 4 of MT. However, they also differ in several important respects, including the fact that the layers of origin in the two areas are different. The V1 projection originates from large pyramids in 5–6 and the spiny stellate and pyramidal cells of layer 4B (Elston and Rosa, 1997), whereas the V2 projection originates mainly from pyramidal cells in layer 3B (Lund et al., 1981; Maunsell and Van Essen, 1983; Ungerleider and Desimone, 1986; Shipp and Zeki, 1989). Unlike the V1 axons, the V2 axons did not innervate the deep layers, and unlike the V1 projection, V2 did innervate the superficial layers, including layer 1. This finding confirms the pattern of the V2 to MT described previously by Rockland (1995). At the ultrastructural level, we discovered that the V2 axons did not form the elaborated and large multisynaptic boutons of the V1 projection to layer 4 (Anderson et al., 1998). The smaller boutons of the V2 projection could reflect a comparatively diminished activity of the V2 vs. the V1 pathway.

In some important respects, the differences between the V1 and V2 projection to MT mirror those of the thalamic projections to V1, where the relay cells in the parvicellular and magnocellular layers of the dorsal lateral geniculate nucleus provide the input to layers 4 and 6 through large multisynaptic boutons (Winfield et al., 1982, Freund et al. 1989), whereas the koniocellular layers project to layers 1–3. As yet, however, we only know a fragment of physiology of the V1 neurons that project to MT and nothing of the neurons that project from V2. In a "rather trying" study, Movshon and Newsome (1996) used antidromic activation to identify 12 V1 neurons projecting to MT. Most

of these neurons were strongly directional, had special complex receptive fields, and were unusually sensitive to low contrast characteristic of the magnocellular pathway. The equivalent study in V2 has yet to be done, but it seems plausible that as with the different thalamocortical streams, each path conveys different aspects of a given stimulus to the target area. The difference in termination pattern would then reflect the differences in local processing required for the given signal, differences in the further destinations of the signal, or both.

If the retrogradely filled cells in V1 included those that project to MT, they might have contributed to the labeling in V2. However, PHA-L or BDA did not give Golgi-like filling of the local axon collaterals of the retrogradely labeled neurons. Together with the above observations of the key differences between the V1 and V2 projections to MT, it was highly unlikely that retrogradely filled cells contributed to the axonal labeling in MT. The proportion of synapses contributed by the injected area in V2 was tiny, only approximately 4–6% of all excitatory synapses in the densest portions of the terminal arbors. However, it is clear that this underestimates the contribution of V2 to MT, because there is extensive convergence of V2 neurons upon MT (Shipp and Zeki, 1985) and our localized injections would label only a subset of these.

The ultrastructural features of the synapses and their targets indicate that the V2 axons in layer 4 form putative excitatory synapses with spiny (putative excitatory) neurons. The electron microscopic analysis showed that, in layer 2/3, there was a decrease in the number of dendritic shafts that were targets. This may simply reflect a different selectivity of the presynaptic axons in the different layers. Alternatively, there may simply be fewer spines in layer 4 with which they can form synapses. Some support for this idea comes from the studies of Elston and Rosa (1997), which indicate that pyramidal cells in layer 3 of MT have larger basal dendrites and slightly higher peak spine densities (7.95 spines/10 μm) than the equivalent layer 3 (4B) pyramids in area 17 (5.79 spines/10 μm). This increased density may provide for more spine targets for the V2 projection to the superficial layers of MT.

The more complicated geometry of the postsynaptic density on spine synapses, which we first noted for the V1 projection to MT, was repeated in the V2 projection, albeit in a less florid form. The reason for the frequent appearance of a doughnut or horseshoe-shaped postsynaptic density on spines, in particular, remains unclear, but one possibility is that it constitutes some optimal geometry for the diffusion of neurotransmitter to both synaptic and possibly extrasynaptically located receptors (see Discussion section in Anderson et al., 1998). Thus, an analysis of the spatial distribution of the various receptor subtypes in these synapses might be fruitful.

The clustering of terminals in layer 4 of the V2 projection is typical of many cortical projections. The projection from V1 to MT also clusters in layer 4 (Rockland, 1989) and so might interdigitate with the V2 projection, but, as yet, there is no evidence for this. Earlier studies on the cells of origin of the V1 projection in layers 4B and 6 indicated that the cells were not clearly organized in slabs or blobs (Lund et al., 1975; Shipp and Zeki, 1989), but recent work of Boyd and Casagrande (1999) does show the projection cells co-aligned with cytochrome blobs in three species, including macaque. The V2 projection to MT arises from clusters of neurons that lie within regions of intense cytochrome oxidase staining, known as the "thick stripes" (Livingstone and Hubel, 1983). MT itself shows indications of clustered physiology in the macaque, e.g., neurons with common direction preference are clustered together (Albright et al., 1984). In MT of the owl monkey, distinct functional and anatomic columns exist for processing local vs. wide field motion (Berezovskii and Born, 2000). This parallelism is a familiar picture in V1 and V2 and evidently is found even in apparently more specialized visual areas like MT.

Although the properties of neurons in different cortical areas have been extensively studied, the role of the multiple interareal connections remains obscure. Rostral visual areas receive convergent projections from the posterior areas, which themselves are extensively interconnected. Thus, for example, area MT receives direct projections from all the caudal visual areas, including V1, V2, V3, V3A, VP, PO, and V4 (see Felleman and Van Essen, 1991). These same areas also receive feedforward connections from their more caudal relations. Neurons in MT, in common with other rostral areas, receive feedforward inputs that are temporally staggered in onset and can be tens to hundreds of msec in duration. The earliest activation is found in V1; subsequently, neurons in V3 and MT become active; and then, even later, neurons in V2 and V4 become active (Raiguel et al., 1989, 1999; Munk et al., 1995; Nowak et al., 1995; Schmolesky et al., 1998).

In all of these areas, the latency and duration of the response also varies according to laminar location of the neurons. Part of the differences of latency of response may be due to conduction times. As yet, the transmission times of the intra-areal axons have only been measured, with difficulty, for the feedforward projection from V1 to MT (Movshon and Newsome, 1996). An additional clue to the conduction times comes from measurements of the diameter and myelination of the axons.

Rockland (1995) commented on the much smaller caliber of the myelinated axons originating in V2 compared with those originating in V1 (~1 μm vs. ~3 μm). The largest pyramidal cells in V1, the Meynert cells, project to MT (Fries et al., 1985) and are likely to have very large axons. Our light microscopic measurements of the diameter of the axons in the white matter beneath MT indicated that, although there are indeed some very large axons, they can arise from both V1 and V2. Sampling from this population indicates that, on entering MT, the V2 axons have similar diameters to the V1 axons (mean diameter: V2 = 1.6 μm, V1 = 1.7 μm). Because a significant length of an axon is also contained in its terminal arbor, where the axons branch extensively and become thinner, the terminal arbor might contribute significantly to the total conduction time. A comparison at electron microscope level of the myelinated portions of the terminal arbors in layer 4 indicated that the diameter of V1 and V2 collaterals were also comparable. Taken altogether, its seems that whatever differences of axon diameter might exist at their source, these differences are virtually washed out by the time the axons reach MT. This finding means that the spread of visual latencies in MT is probably more due to the times of processing within the antecedent visual areas and not in the transmission times.

The role of the multiple projections to single extrastriate cortical areas remains speculative. Of course, it is

supposed that the different streams bring different components to the computation being carried out by local circuits. Functionally, however, it has been difficult to separate out the different sources of input to MT. When the input to MT from V1 is removed, by ablation (Rodman et al., 1990) or cooling (Girard et al., 1992), some function remains. However, this residual function cannot be carried by the V2 projection, because V2 itself is silenced by inactivation of V1 (Schiller and Malpeli, 1977; Girard and Bullier, 1989), thus, it is possible that the V2 projection to MT provides some overlapping functions with the projection from V1.

Interesting evidence for the V2 pathway to MT has emerged from human studies. For example, Vaina et al. (2000) have studied a patient with a selective lesion in V2. He was found to be impaired in several motion tasks, including those involving first order, but not second-order motion. One possible interpretation is that the loss of the V2 input to MT produces this effect. One human model that uses the V2 connection as the major drive to MT is that of Friston and Buchel (2000). Their evidence from human functional magnetic resonance imaging was that the hemodynamic responses recorded in the human MT and in posterior parietal cortex are enhanced by attention during visual motion, but the responses in pulvinar and V2 are not. They proposed a model in which the connection between V2 and MT was modulated by afferents of the parietal cortex. In their model, V2 and pulvinar provided "driving" inputs to MT, whereas the posterior parietal cortex provided an attentional signal that augmented the V2 input in a nonlinear way. Their model indicates that the activity in the posterior parietal cortex could account for a significant component of the V5 responses under conditions of attention. In this model, the V2 afferents have no different role from "driving" inputs from any other cortical area, e.g., V1. Nevertheless, such models offer a means of exploring this interesting question in other primate species.

LITERATURE CITED

Ahmed B, Anderson JC, Martin KAC, Nelson JC. 1997. Map of the synapses onto layer 4 basket cells of the primary visual cortex of the cat. J Comp Neurol 380:230–242.

Albright TD, Desimone R, Gross CG. 1984. Columnar organization of directionally-selective cells in visual area MT of macaques. J Neurophysiol 51:16–31.

Anderson JC, Binzegger T, Martin KAC, Rockland KS. 1998. The connection from cortical area V1 to V5: a light and electron microscopic study. J Neurosci 18:10525–10540.

Barone P, Batardiere A, Knoblauch K, Kennedy H. 2000. Laminar distribution of neurons in extrastriate areas projecting to visual area V1 and V4 correlates with the hierarchical rank and indicates the operation of a distance rule. J Neurosci 20:3263–3281.

Berezovskii VK, Born RT. 2000. Specificity of projections from wide-field and local motion-processing regions within the middle temporal visual area of the owl monkey. J Neurosci 20:1157–1169.

Boyd JD, Casagrande VA. 1999. Relationship between cytochrome oxidase (CO) blobs in primate primary visual cortex (V1) and the distribution of neurons projecting to the middle temporal area (MT). J Comp Neurol 409:573–591.

Elston GN, Rosa GP. 1997. The occipitoparietal pathway of the macaque monkey: comparison of pyramidal cell morphology in layer 3 of functionally related cortical visual areas. Cereb Cortex 7:432–452.

Felleman DJ, Van Essen DC. 1991. Distributed hierarchical processing in the primate cerebral cortex. Cereb Cortex 1:1–47.

Freund TF, Martin KAC, Soltesz P, Somogyi P, Whitteridge D. 1989. Arborization patterns and postsynaptic targets of physiologically identified thalamocortical afferents in striate cortex of the macaque monkey. J Comp Neurol 289:315–336.

Friedman DP. 1983. Laminar patterns of termination of corticocortical afferents in the somatosensory system. Brain Res 273:147–151.

Fries W, Keizer K, Kuypers HG. 1985. Large layer VI cells in macaque striate cortex (Meynert cells) project to both superior colliculus and prestriate visual area V5. Exp Brain Res 58:613–616.

Friston KJ, Buchel C. 2000. Attentional modulation of effective connectivity from V2 to V5/MT in humans. Proc Natl Acad Sci U S A 97:7591–7596.

Girard P, Bullier J. 1989. Visual activity in area V2 during reversible inactivation of area 17 in the macaque monkey. J Neurophysiol 62: 1287–1302.

Girard P, Salin PA, Bullier J. 1992. Response selectivity of neurons in area MT of the macaque monkey during reversible inactivation of area V1. J Neurophysiol 67:1437–1446.

Jouve B, Rosenstiehl P, Imbert M. 1998. A mathematical approach to the connectivity between the cortical visual areas of the macaque monkey. Cereb Cortex 8:28–39.

Kennedy H, Bullier J. 1985. Double-labeling investigation of the afferent connectivity to cortical areas V1 and V2 of the macaque monkey. J Neurosci 10:2815–2830.

Kisvárday ZF, Martin KAC, Whitteridge D, Somogyi P. 1985. Synaptic connections of intracellularly filled clutch neurons, a type of small basket neuron in the visual cortex of the cat. J Comp Neurol 241:111–137.

Livingstone MS, Hubel DH. 1983. Specificity of cortico-cortical connections in monkey visual system. Nature 304:531–534.

Lund JS, Lund RD, Hendrickson AE, Bunt AH, Fuchs AF. 1975. The origin of efferent pathways from the primary visual cortex, area 17, of the macaque monkey as shown by retrograde transport of horseradish peroxidase. J Comp Neurol 164:287–303.

Lund JS, Hendrickson AE, Ogren MP, Tobin EA. 1981. Anatomical organization of primate visual cortical area VII. J Comp Neurol 202:19–45.

Maunsel JH, Van Essen DC. 1983. The connections of the middle temporal visual area (MT) and their relationship to a hierarchy in the macaque. J Neurosci 3:2563–2586.

Movshon JA, Newsome WT. 1996. Visual response properties of striate cortical neurons projecting to area MT in macaque monkeys. J Neurosci 16:7733–7741.

Munk M, Nowak L, Girard P, Chounlamountri N, Bullier J. 1995. Visual latencies in cytochrome oxidase bands of macaque area V2. Proc Natl Acad Sci U S A 92:988–992.

Nowak LG, Munk MH, Girard P, Bullier J. 1995. Visual latencies in areas V1 and V2 of the macaque monkey. Vis Neurosci 12:371–384.

Peters A, Saint Marie RL. 1984. Smooth and sparsely spinous nonpyramidal cells forming local axonal plexuses. In: Jones EG, Peters A, editors. Cerebral cortex. Vol. 1. Cellular components of the cerebral cortex. New York: Plenum Press. p 419–445.

Peters A, Palay SL, Webster HD. 1991. The fine structure of the nervous system: neurons and their supporting cells. 3rd ed. Oxford: Oxford University Press.

Raiguel SE, Lagae L, Gulyas B, Orban GA. 1989. Response latencies of visual cells in macaque areas V1, V2 and V5. Brain Res 493:155–159.

Raiguel SE, Xiao DK, Marcar VL, Orban GA. 1999. Response latency of macaque area MT/V5 neurons and its relationship to stimulus parameters. J Neurophysiol 82:1944–1956.

Rockland KS. 1989. Bistratified distribution of terminal arbors of individual axons projecting from area V1 to middle temporal area (MT) in the macaque monkey. Vis Neurosci 3:155–170.

Rockland KS. 1995. Morphology of individual axons projecting from area V2 to MT in the macaque. J Comp Neurol 355:15–26.

Rockland KS, Pandya DN. 1979. Laminar origins and terminations of cortical connections of the occipital lobe in the rhesus monkey. Brain Res 179:3–20.

Rodman HR, Gross CG, Albright TD. 1990. Afferent basis of visual response properties in area MT of the macaque. II. Effects of superior colliculus removal. J Neurosci 10:1154–1164.

Schmolesky MT, Wang Y, Hanes DP, Thompson KG, Leutgeb S, Schall JD, Leventhal AG. 1998. Signal timing across the macaque visual system. J Neurophysiol 79:3272–3278.

Schiller PH, Malpeli JG. 1977. The effect of striate cortex cooling on area 18 cells in the monkey. Brain Res 126:366–369.

Shipp S, Zeki S. 1985. Segregation of pathways leading from area V2 to areas V4 and V5 of macaque monkey visual cortex. Nature 315:322–325.

Shipp S, Zeki S. 1989. The organization of connections between area V5 and V1 in macaque monkey visual cortex. Eur J Neurosci 1:309–332.

Somogyi P, Kisvárday ZF, Martin KAC, Whitteridge D. 1983. Synaptic connections of morphologically identified and physiologically characterized large basket cells in the striate cortex of cat. Neuroscience 10:261–294.

Sporns O, Tononi G, Edelman GM. 2000. Theoretical neuroanatomy: relating anatomical and functional connectivity in graphs and cortical connection matrices. Cereb Cortex 10:127–141.

Sterio DC. 1984. The unbiased estimation of number and sizes of arbitrary particles using the disector. J Microsc 134:127–136.

Ungerleider LG, Desimone R. 1986. Cortical connections of visual area MT in the macaque. J Comp Neurol 248:190–222.

Vaina LM, Soloviev S, Bienfang DC, Cowey A. 2000. A lesion of cortical area V2 selectively impairs the perception of the direction of first-order visual motion. Neuroreport 7:1039–1044.

Winfield DA, Rivera-Dominguez M, Powell TPS. 1982. The termination of geniculocortical fibres in area 17 of the visual cortex in the macaque monkey. Brain Res 231:19–32.

Young MP. 1992. Objective analysis of the topological organization of the primate cortical visual system. Nature 358:152–155.